ELSEVIER

Contents lists available at ScienceDirect

Free Radical Biology and Medicine

journal homepage: www.elsevier.com/locate/freeradbiomed





Quantitation of oxidized nuclear and mitochondrial DNA in plasma samples of patients with abdominal aortic aneurysm

Hubert Hayden ^a, Johannes Klopf ^a, Nahla Ibrahim ^a, Viktoria Knöbl ^a, Anna Sotir ^a, Ronald Mekis ^b, Karin Nowikovsky ^b, Wolf Eilenberg ^a, Christoph Neumayer ^a, Christine Brostjan ^a, ^{*}

- ^a Department of General Surgery, Division of Vascular Surgery, Medical University of Vienna and University Hospital Vienna, Waehringer Guertel 18-20, 1090, Vienna, Austria
- b Institute of Physiology, Pathophysiology and Biophysics, Unit of Physiology and Biophysics, University of Veterinary Medicine, 1210, Vienna, Austria

ARTICLE INFO

Keywords:
8-oxo-7,8-dihydro-2'-deoxyguanosine
8-oxodGuo
Alu element
Immunoprecipitation
MT-ND5
Oxidized DNA
Plasma
Quantitative polymerase chain reaction

ABSTRACT

There is accumulating evidence that pro-inflammatory features are inherent to mitochondrial DNA and oxidized DNA species. 8-oxo-7,8-dihydro-2'-deoxyguanosine (8-oxodGuo) is the most frequently studied oxidatively generated lesion. Modified DNA reaches the circulation upon cell apoptosis, necrosis or neutrophil extracellular trap (NET) formation. Standard chromatography-based techniques for the assessment of 8-oxodGuo imply degradation of DNA to a single base level, thus precluding the attribution to a nuclear or mitochondrial origin. We therefore aimed to establish a protocol for the concomitant assessment of oxidized mitochondrial and nuclear DNA from human plasma samples. We applied immunoprecipitation (IP) for 8-oxodGuo to separate oxidized from non-oxidized DNA species and subsequent quantitative polymerase chain reaction (qPCR) to assign them to their subcellular source. The IP procedure failed when applied directly to plasma samples, i.e. isotype control precipitated similar amounts of DNA as the specific 8-oxodGuo antibody. In contrast, DNA isolation from plasma prior to the IP process provided assay specificity with little impact on DNA oxidation status. We further optimized sensitivity and efficiency of qPCR analysis by reducing amplicon length and targeting repetitive nuclear DNA elements. When the established protocol was applied to plasma samples of abdominal aortic aneurysm (AAA) patients and control subjects, the AAA cohort displayed significantly elevated circulating non-oxidized and total nuclear DNA and a trend for increased levels of oxidized mitochondrial DNA. An enrichment of mitochondrial versus nuclear DNA within the oxidized DNA fraction was seen for AAA patients. Regarding the potential source of circulating DNA, we observed a significant correlation of markers of neutrophil activation and NET formation with nuclear DNA, independent of oxidation status. Thus, the established method provides a tool to detect and distinguish the release of oxidized nuclear and mitochondrial DNA in human plasma and offers a refined biomarker to monitor disease conditions of pro-inflammatory cell and tissue destruction.

1. Introduction

Life in an oxygenated environment entails damage to organic compounds including DNA [1]. Oxidative damage can occur to all nucleobases but guanine is particularly prone to oxidation [2,3]. 8-oxo-7, 8-dihydro-2'-deoxyguanosine (8-oxodGuo) is the most frequently investigated oxidatively generated lesion [3]. If not repaired, 8-oxodGuo may cause mutations, since it can erroneously pair with adenine instead of cytosine [4]. Apart from single base modifications, interstrand

crosslinks as well as DNA-protein crosslinks can occur upon oxidative DNA damage [2].

Since reactive oxygen species (ROS) are a central element of our immune strategy, oxidized DNA is often observed during pathogen defense or in pathological conditions of inflammation. Thus, levels of circulating oxidized DNA have been assessed in the context of disease. Serum 8-oxodGuo is elevated in patients with peripheral artery disease (PAD) compared to healthy controls and is reduced by intake of an antioxidant supplement [5]. Occurrence and severity of coronary artery

E-mail address: christine.brostjan@meduniwien.ac.at (C. Brostjan).

^{*} Corresponding author. Department of General Surgery, Division of Vascular Surgery, Medical University of Vienna and University Hospital Vienna, Anna Spiegel Center for Translational Research, 25.05.002, Waehringer Guertel 18-20, 1090, Vienna, Austria.

disease (CAD) are associated with serum 8-oxodGuo levels [6]. Moreover, a meta-analysis confirmed increased blood 8-oxodGuo in patients with cardiovascular disease (including patients suffering from CAD, stroke, carotid atherosclerosis and PAD) compared to controls [7]. Apart from cardiovascular disease, the analysis of circulating oxidized DNA has further been of interest with regard to neoplastic conditions [8,9], neurological disorders [10] and autoimmune conditions [11]. Of note, levels of circulating DNA oxidation products were also shown to be altered after extensive physical exercise [12].

Various mechanisms may result in the release of oxidized DNA or nucleotides into circulation. Upon cell death by necrosis or apoptosis, DNA can be transferred into circulation [13] and apoptotic bodies are known to carry DNA cargo [14]. Furthermore, DNA contained in exosomes is also detectable in plasma [15]. A particular mode of DNA release has been discovered more recently: Neutrophil extracellular trap (NET) formation was described as a mechanism to arrest and kill pathogens. It is characterized by the expulsion of neutrophil DNA into the extracellular space, which is decorated with granule proteins, antimicrobial compounds and histones [16]. Since ROS production is a central feature of neutrophil activation and NET formation, NET DNA is prone to carry oxidative alterations such as 8-oxodGuo [17,18]. While both, nuclear and mitochondrial DNA may be expelled during NET formation [17,19], mitochondrial DNA is considered to be more sensitive to oxidative damage due to lack of protection by histones, lower repair capabilities and its vicinity to ROS production by the respiratory chain [17,20,21]. Thus, NET formation can substantially contribute to the pool of circulating oxidized DNA, in particular of mitochondrial origin.

Of note, most studies investigating oxidized DNA in circulation have focused on lesions at a single nucleobase level rather than incorporated into a DNA strand. Standard methods for the assessment of oxidized nucleobases and their derivatives (including 8-oxodGuo) comprise various chromatography techniques such as high performance liquid chromatography (HPLC) or gas chromatography in combination with electrochemical detection [22] or (tandem) mass spectrometry (MS/MS) [23,24]. At a single cell level, gel electrophoresis (also termed "comet assay") is used in combination with enzymes recognizing oxidatively generated lesions [25]. Enzyme-based techniques are generally more sensitive than chromatographic procedures but exhibit a low detection range [26,27]. Of note, chromatographic methods were found to detect substantially higher levels of DNA oxidation than enzymatic assays, indicating susceptibility to spurious base modification during sample handling [27]. Yet for both, enzymatic and chromatographic approaches, the inter-laboratory reproducibility is poor as the determined levels of oxidatively modified DNA may vary up to 10-fold [26,28]. Alternatively, antibody based techniques like immunohistochemistry [29], immunofluorescence [17,23] and enzyme-linked immunosorbent assay (ELISA) [5,6,17] have been applied. In a direct comparison, chromatography based assays were found to be more accurate in determining urinary levels of 8-oxodGuo than ELISAs, since the latter revealed a higher level of variability and tended to overestimate absolute contents [30]. Thus, HPLC followed by electrospray ionization and MS/MS has been proposed for measuring oxidatively generated lesions [2], but requires specialized equipment and knowledge and does not allow for the distinction of nuclear versus mitochondrial DNA damage.

There is accumulating evidence that in particular the mitochondrial DNA and oxidized DNA species trigger pro-inflammatory responses. For example, intra-articular injection of mitochondrial, but not nuclear DNA, induces joint inflammation [20]. However, when a single 8-oxodGuo molecule is incorporated into an oligodeoxynucleotide stretch, this leads to a massive elevation of arthritis frequency compared to the unmodified molecule [20]. Self as well as foreign DNA molecules harboring 8-oxodGuo are more easily sensed due to a delayed destruction by cytosolic DNase III [31]. This results in an enhanced IFN alpha (IFN- α) response, correlating with the amount of incorporated 8-oxodGuo. Accordingly, oxidized DNA originating from neutrophils and NETs is proposed to act as a damage-associated molecular pattern

triggering IFN- α secretion from monocytes, macrophages or dendritic cells [31,32]. In patients with systemic lupus erythematosus (SLE), the levels of circulating mitochondrial DNA were found to be significantly higher than in healthy controls and correlated with disease activity [32]. Lood *et al.* reported that SLE patients had a higher propensity to expel NETs enriched in oxidized mitochondrial DNA and that particularly the oxidized as opposed to the non-oxidized DNA (independent of its nuclear or mitochondrial origin) had pro-inflammatory i.e. interferogenic capacity [17].

Considering the increasing number of reports on NET involvement in cardiovascular, autoimmune, neoplastic and other diseases [33], we inferred that a reliable and rapid detection method for oxidized nuclear and mitochondrial DNA in patient blood might lead to biomarkers suitable for disease monitoring. Thus, we hypothesized that levels of circulating oxidized DNA are elevated in cardiovascular pathologies associated with NET formation such as atherosclerosis [34], thrombosis [35] or abdominal aortic aneurysm (AAA) [36-40]. In this study, we first aimed to establish a protocol for the concomitant assessment of oxidized mitochondrial and nuclear DNA from blood specimens. For this purpose, we adopted a basic protocol applied by Lood and co-workers for the analysis of 8-oxodGuo positive DNA in culture supernatant of isolated neutrophils [17] and optimized it for human plasma samples, discriminating between cell-free oxidized DNA of mitochondrial and nuclear origin. The final protocol was then applied to plasma samples of AAA patients and controls and the established levels of oxidized mitochondrial and nuclear DNA were compared with markers of neutrophil activation and NET formation to assess their potential association.

2. Materials and methods

2.1. Cell isolation and cell culture

Neutrophil granulocytes were isolated from ethylenediaminetetraacetic acid anticoagulated peripheral blood similar to a previously published protocol [41] based on density gradient centrifugation with Histopaque®-1119 (Sigma-Aldrich, St. Louis, MO) and Ficoll®-Paque Plus (GE Healthcare, Chicago, IL) followed by hypotonic erythrocyte lysis [42]. Isolated cells were resuspended in phosphate-buffered saline (PBS) without calcium and magnesium (Thermo Fisher Scientific, Waltham, MA), counted with a Sysmex XN-350 device (Sysmex, Kobe, Japan) and frozen at -80 °C or immediately subjected to DNA isolation. The cell line 143B206 served as a classical mitochondrial DNA-less (ρ^0) cell system. Briefly, these cells were originally isolated by King and Attardi from the parental thymidine kinase-negative (TK⁻) human osteosarcoma cell line 143B (ATCC CRL-8303) grown in the presence of 50 ng/ml ethidium bromide, which inhibits mitochondrial DNA replication and thus over an extended period of time completely depletes mitochondrial DNA [43]. Since cells lacking mitochondrial DNA are auxotrophic, the 143B206 cell line was propagated in the presence of 1 mg/ml sodium pyruvate (Thermo Fisher Scientific) and 50 μg/ml uridine (Merck, Darmstadt, Germany). The parental 143B.TK cells served as mitochondrial DNA positive controls, and cell pellets of 143B.TK and 143B.TK⁻ ρ^0 cells (143B206) were applied to subsequent DNA isolation.

2.2. DNA isolation from cells

DNA isolation, either from 5×10^6 isolated neutrophils, 2.5×10^6 143B.TK $^-$ cells or 2.5×10^6 143B.TK $^ \rho^0$ cells was performed with DNeasy Blood & Tissue Kit (Qiagen, Venlo, The Netherlands) applying the "spin-column protocol for purification of total DNA from animal blood or cells". Briefly, cells were resuspended in 190 μ l of PBS without calcium and magnesium, then supplemented with 20 μ l of proteinase K (kit component), followed by 200 μ l of buffer AL (kit component). Samples were incubated for 10 min at 56 °C to allow for cell disruption and protein digestion. Subsequent to the addition of 200 μ l of absolute

ethanol (Merck), samples were transferred onto DNeasy mini spin columns (kit component). After washing the columns with buffers AW1 and AW2 (kit components), neutrophil DNA was eluted by application of two consecutive fractions of 100 μl of nuclease-free water (NFW, component of GoTaq® qPCR Master Mix Kit, Promega, Madison, WI) which were pooled after elution, while DNA from 143B.TK $^-$ cells and 143B.TK $^-$ ocells was eluted with a single fraction of 100 μl AE buffer (component of DNeasy Blood & Tissue Kit).

2.3. DNA isolation from plasma

DNA isolation from 190 μ l of citrate plasma was performed with DNeasy Blood & Tissue Kit as specified for cells, but DNA was finally eluted with 30 μ l of NFW or 30 μ l of AE buffer when prepared for immunoprecipitation (IP) or quantitative polymerase chain reaction (qPCR) analysis, respectively. In either case, the volume was applied trice to the same spin column to enhance DNA yield. Where indicated, DNA was isolated from 190 μ l of citrate plasma with the alternatively tested QIAamp DSP DNA Blood Mini Kit (Qiagen) according to the manufacturer's microcentrifuge protocol and eluted with 30 μ l of buffer AE (kit component, applied trice).

2.4. Protein G-based immunoprecipitation

Our initial IP protocol mainly followed a previously published method [17] using a commercially available protein G based IP kit (DynabeadsTM Protein G Immunoprecipitation Kit, Thermo Fisher Scientific). For each IP, 25 µl (equal to 0.75 mg) of resuspended microbeads were transferred into a 1.5 ml polypropylene centrifugation tube. With the support of a magnetic tool (Dynal MPC®-E, Thermo Fisher Scientific), the buffer was removed and the beads were then coupled with 6 μ g of antibody diluted in 100 µl of antibody binding and washing buffer (component of DynabeadsTM Protein G Immunoprecipitation Kit). The following antibodies were used: mouse anti-DNA/RNA damage monoclonal antibody (clone 15A3, IgG_{2b} , targeting 8-oxodGuo as well as 8-oxo-7,8-dihydroguanine [8-oxoGua] and 8-oxo-7,8-dihydroguanosine [8-oxoGuo] [44], no. SMC-155D, StressMarq Biosciences, Victoria, Canada) or mouse IgG_{2b} monoclonal isotype control (clone 20116, no. MAB004, Bio-Techne, Minneapolis, MN). Where indicated, the antibody was omitted during the binding procedure (for control purposes). Antibody coupling was performed for 10 min at room temperature under constant rotation. The unbound material was then removed and the beads were washed three times with 100 µl of washing buffer (component of DynabeadsTM Protein G Immunoprecipitation Kit), followed by one wash with 100 µl of antibody binding and washing buffer. Sample (190 µl of citrate plasma or isolated neutrophil DNA) was subjected to immunoprecipitation in two consecutive steps: First, 95 µl of sample were added to the beads and IP was performed for 2 h under constant rotation (with an additional, brief manual resuspension after 1 h). The unbound material was then collected in a fresh centrifugation tube while the remaining 95 µl of sample were added to the same microbeads. Now IP was performed overnight at 4 °C under constant rotation (with an additional resuspension after 2 h). The unbound material was again removed and combined with the unbound fraction of the first IP round (for subsequent isolation of the non-oxidized DNA). Finally, the beads were washed three times with 100 µl of washing buffer. To avoid interference from plastic-bound DNA, the microbeads were transferred into a new centrifugation tube with 100 µl of fresh washing buffer. The supernatant was again removed and the beads were resuspended with 190 µl of PBS without calcium and magnesium and immediately subjected to DNA isolation (of the oxidized DNA fraction).

2.5. Streptavidin-based immunoprecipitation

An alternative method of immunoprecipitation based on biotin-conjugated antibodies was established. For each IP, 25 μ l (equal to

0.25 mg) of resuspended PierceTM Streptavidin Magnetic Beads (Thermo Fisher Scientific) were transferred into a 1.5 ml polypropylene centrifugation tube. With the support of a Dynal MPC®-E magnetic device, the buffer was removed and the beads were washed three times with 150 μl of self-prepared binding/wash buffer. Binding/wash buffer was composed (as recommended in the PierceTM Streptavidin Magnetic Beads datasheet) of 25 mM tris(hydroxymethyl)aminomethane, 150 mM NaCl, 0.1% TWEEN® 20 and adjusted to pH 7.2 with hydrochloric acid (all reagents by Merck). Prepared beads were then coupled with $5 \mu g$ of antibody diluted in $100~\mu l$ of binding/wash buffer. The following antibodies were applied: biotinylated mouse anti-DNA/RNA damage monoclonal antibody (clone 15A3, IgG_{2b} , no. SMC-155D-BI, StressMarq Biosciences) or biotinylated mouse IgG_{2b} monoclonal isotype control (clone MPC-11, no. HI1023, Hycult Biotech, Uden, The Netherlands). Where indicated, the antibody was omitted during the binding procedure (for control purposes). Antibody coupling was performed for 60 min at room temperature under constant rotation with additional manual resuspension every 20 min. The non-bound material was then removed and the beads were washed once with 150 µl of binding/wash buffer. Sample (isolated DNA diluted in 190 µl PBS without calcium and magnesium) was added and the IP was performed under constant rotation in two steps, as specified for the protein G based IP procedure. The unbound material (non-oxidized DNA) was transferred to a fresh centrifugation tube for subsequent DNA isolation. The collected beads were washed three times with 150 µl of binding/wash buffer. To avoid interference from plastic-bound DNA, the microbeads were transferred to a new centrifugation tube with 150 µl of fresh binding/wash buffer. The supernatant was again removed and the beads were resuspended with 190 µl of PBS without calcium and magnesium and immediately subjected to isolation of the oxidized DNA fraction.

2.6. DNA isolation from IP material

DNA isolation from antibody/bead-bound (i.e. the oxidized or 8-oxodGuo positive DNA fraction) and unbound (i.e. the non-oxidized or 8-oxodGuo negative DNA fraction) IP material was performed with DNeasy Blood & Tissue Kit (Qiagen, Venlo, The Netherlands) as specified for cells, taking the following details into account. After addition of absolute ethanol, the microbeads in the antibody/bead-bound fraction were separated from the liquid using a Dynal MPC®-E magnetic device. Oxidized and non-oxidized DNA was eluted with 30 μl of buffer AE which was applied trice to the same spin column to optimize yield.

2.7. Quantitative polymerase chain reaction

Nuclear and mitochondrial DNA sequences were detected and quantified by means of SYBR Green based qPCR using GoTaq® qPCR Master Mix Kit (Promega) as follows. Unless otherwise stated, 2 µl of eluted DNA as template were mixed with GoTag® qPCR Master Mix (kit component, 1x final concentration), CXR reference dye (kit component, 0.3 µM final concentration), appropriate forward and reverse primers (see Supplementary Table 1 for sequences and final concentrations) and NFW (kit component) in a total volume of 20 µl per reaction. No template control (NTC) samples, omitting template DNA, were additionally assayed on each plate. All primers were synthesized by Eurofins Genomics (Ebersberg, Germany) in HPLC-purified quality. Samples were distributed into MicroAmp™ Fast Optical 96-Well Reaction Plates (Thermo Fisher Scientific) and sealed with MicroAmpTM Optical Adhesive Film (Thermo Fisher Scientific). Real-time detection of amplified DNA was performed with a 7500 Fast Real-Time PCR System (Thermo Fisher Scientific) equipped with 7500 software version 2.3 (Thermo Fisher Scientific) using the following settings: 2 min at 50 $^{\circ}$ C, then 10 min at 95 $^{\circ}\text{C}$ followed by 45 cycles, each consisting of 15 s at 95 $^{\circ}\text{C}$ plus 1 min at 60 °C. To assess amplicon uniformity, melting curves were recorded upon slow and gradual heating from 60 °C to 95 °C. Reaction conditions resulting in PCR products with an aberrant melting profile (i.

e. with a peak shift or two or more peaks) were excluded from further analysis. To obtain cycle threshold (ct) values, the threshold was manually set to 0.1 Δ Rn for each applied primer pair. For primer characterization, slope and regression coefficient (R²) were calculated with serially diluted isolated neutrophil or plasma DNA templates using 7500 software (Thermo Fisher Scientific). Primer efficiencies were calculated according to the following equation (1):

Primer efficiency =
$$10^{-(1/\text{slope})}$$
 (1)

Unless otherwise stated, the relative content of detected nuclear or mitochondrial DNA sequence was calculated according to the following equation (2):

DNA content = primer efficiency
$$^{\text{ct calibrator - ct sample}}$$
 (2)

During protocol optimization, the calibrator ct was arbitrarily set to 40.0, whereas for the observational AAA study, the ct value of an internal calibrator (applied to each qPCR plate) was used to determine the normalized amount of oxidized and non-oxidized mitochondrial and nuclear DNA. Thus, by definition, the internal calibrator was set to a DNA content of 1.0 while samples displaying no amplification were set to 0.0. Total DNA amounts (of either mitochondrial or nuclear origin) and the percentage of oxidized DNA were calculated according to the following equations: total amount of DNA = normalized amount of oxidized DNA+ normalized amount of non-oxidized DNA; percentage of oxidized DNA = (normalized amount of oxidized DNA/total amount of DNA) x 100. To set the oxidized mitochondrial and nuclear DNA into relation, the following formula was applied: ratio = percentage of oxidized mitochondrial DNA/percentage of oxidized nuclear DNA.

2.8. Preparation of internal calibrator

With regard to the observational AAA study, an internal calibrator was prepared for DNA content calculation and for normalization between different qPCR plates. To this end, DNA was isolated from citrate plasma of 20 different AAA patients. The DNA was pooled and stored at $-80\,^{\circ}\mathrm{C}$ in appropriate aliquots until further use. The internal calibrator was applied to each qPCR plate.

2.9. Observational AAA study design

Thirty-nine advanced AAA patients without surgical aneurysm repair (recruited at the Vascular Surgery outpatient clinic of the University Hospital Vienna) and 39 controls (recruited among General Surgery, Urology and Ophthalmology patients presenting for routine examinations) were included into an observational case-control study between 2014 and 2016. Patients and controls were matched for sex, age, body mass index (BMI) and smoking habit. Maximum aortic diameter of AAA patients was determined by computed tomography angiography scan, whereas the absence of AAA in controls was verified by ultrasound examination. The study was approved by the institutional ethics committee of the Medical University of Vienna (license number 1729/2014) and registered at https://www.researchregistry.com (unique identifying number 7647). Written informed consent was given by all study participants prior to blood withdrawal and their demographics were recorded by means of a structured questionnaire. The study was performed in accordance with the principles of the Declaration of Helsinki and the STROBE guidelines.

2.10. Plasma preparation and assessment of neutrophil markers

Upon study inclusion, citrate anticoagulated peripheral blood was collected and processed within 60 min. To obtain platelet-free plasma, blood was centrifuged twice (1000×g followed by 10 000×g, both 10 min at 4 $^{\circ}\text{C}$) and stored at -80 $^{\circ}\text{C}$ in aliquots. Plasma myeloperoxidase (MPO, Human Myeloperoxidase Quantikine ELISA Kit, Bio-Techne) and

DNA-histone complexes (Cell Death Detection ELISA, Merck) were assessed according to the manufacturer's recommendations. Plasma neutrophil elastase (NE) and neutrophil gelatinase-associated lipocalin (NGAL) levels were quantified with the Human Sepsis Magnetic Bead Panel 3 (EMD Millipore, Billerica, MA) in a Luminex MagPix instrument (Thermo Fisher Scientific). Citrullinated histone H3 (citH3) was measured as previously reported [45,46]. Biochemical blood parameters were determined by the University Hospital Vienna routine laboratory. Differential blood count was assessed with a Sysmex XN-350 device.

2.11. Statistical analysis

With regard to the observational AAA study, nominal variables are indicated as counts and percent of sample group. They were statistically evaluated for differences by means of Chi square or Fisher exact test. Continuous variables are presented with median and interquartile range (IQR) and were assessed with non-parametric tests (i.e. Mann-Whitney U test with respect to group comparisons and Spearman's coefficient r_s for correlations). Continuous variables are depicted with boxplots (visualizing group comparisons) or scatterplots (visualizing correlations). To analyze the diagnostic biomarker value of the investigated DNA parameters for the presence of AAA in relation to other co-morbidities, multivariable analysis (binary logistic regression, method Enter) was performed by including all variables with a significance level <0.1 in univariable analysis. Statistical evaluation was conducted with SPSS Statistics 27.0 software (IBM, Armonk, NY) and statistical tests were reported as significant when a two-sided p-value <0.05 was calculated.

3. Results

3.1. IP-based detection of oxidized DNA in human plasma requires DNA purification prior to immunoprecipitation

We aimed to establish an IP-based method for the detection of 8oxodGuo carrying DNA in human plasma and subsequent distinction of mitochondrial versus nuclear origin by qPCR. While a previously published protocol with protein G coated microbeads for neutrophil supernatants [17] was readily applicable to isolated neutrophil DNA (Supplementary Figs. 1a and b), assay specificity was lost for plasma samples (Supplementary Figs. 1c and d), as isotype antibody or uncoupled beads precipitated comparable (and very low) amounts of DNA as the 8-oxodGuo antibody. Similarly, a streptavidin-biotin based system for the immobilization of IP antibodies to the solid phase did not eliminate the unspecific precipitation of plasma DNA by control antibody or uncoupled beads (Supplementary Figs. 2a and b). Furthermore, the specific detection of oxidized DNA was lost when isolated neutrophil DNA was spiked into human plasma (Supplementary Figs. 2c and d). As little as 10% (v/v) plasma impaired the detection of oxidized neutrophil DNA and the effect was particularly pronounced for mitochondrial DNA (Supplementary Figs. 2e and f). However, the detection of oxidized DNA could be rescued by isolation of DNA from plasma prior to the immunoprecipitation procedure: When isolated neutrophil DNA was spiked at high levels into human plasma and then subjected to re-extraction, the detected percentage of oxidized mitochondrial DNA was stable and the absolute amount and percentage of oxidized nuclear DNA were only minimally increased (Fig. 1, Supplementary Table 2). Of note, the purification of DNA from plasma resulted in a detectable loss of mitochondrial DNA, which was comparable for neutrophil DNA incubated with plasma overnight or immediately subjected to re-extraction (Fig. 1, Supplementary Table 2). Application of different IP buffer systems did not affect the DNA oxidation status but also documented that mitochondrial rather than nuclear DNA was partly lost during the IP procedure (Supplementary Table 3).

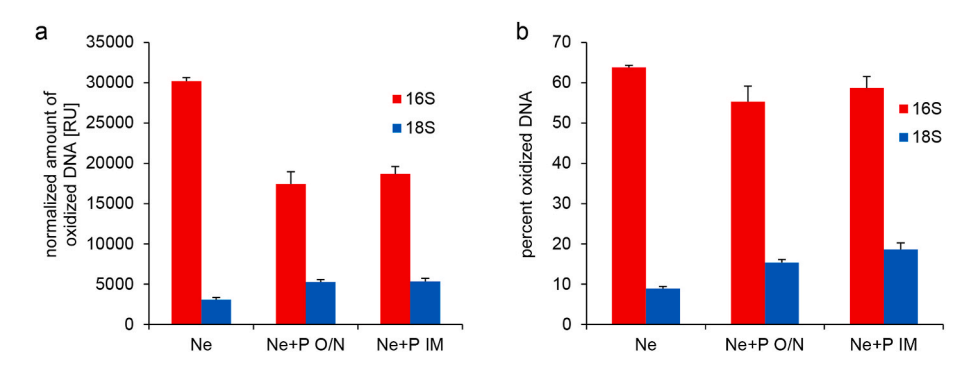


Fig. 1. DNA oxidation is moderately affected by exposure to plasma. Streptavidin coated microbeads were coupled with biotinylated antibodies against 8oxodGuo. DNA was isolated from neutrophils and 1000 ng were directly subjected to the IP process (Ne). Alternatively, 1000 ng of isolated neutrophil DNA were added to citrate plasma (final plasma concentration: 84% [v/v]) and re-extracted after overnight incubation (Ne + P O/N) or immediately after mixing (Ne + P IM). The retrieved material (584 ng or 535 ng DNA for Ne + P O/N or Ne + P IM, respectively) was subjected to the streptavidin-based IP protocol. Precipitated (8-oxodGuo positive fraction) and non-precipitated (8-oxodGuo negative fraction) material underwent a further round of DNA isolation and subsequent aPCR with primers targeting

16S and 18S. A) The normalized amount of oxidized DNA or b) the percent oxidized DNA is illustrated. Mean \pm SD represent technical qPCR replicates (n = 3). RU, relative units.

3.2. Sensitive detection of nuclear and mitochondrial DNA from human plasma is facilitated by short qPCR amplicons and repetitive DNA elements

Since nuclear and mitochondrial DNA fragments in plasma are reportedly short [47,48], we aimed to improve detection sensitivity by reducing amplicon length and altering target gene sequences in qPCR

analysis. Originally, primer sets for 16S and 18S ribosomal RNA were adopted from a published protocol [17] covering DNA sequences of 103 and 151 bp, respectively and exhibiting moderate primer efficiencies in the range of 1.7. Among the tested alternatives for mitochondrial genes (MT-CO2, MT-ND5), in particular the primer set for MT-ND5 displayed increased sensitivity compared to 16S detection (Supplementary

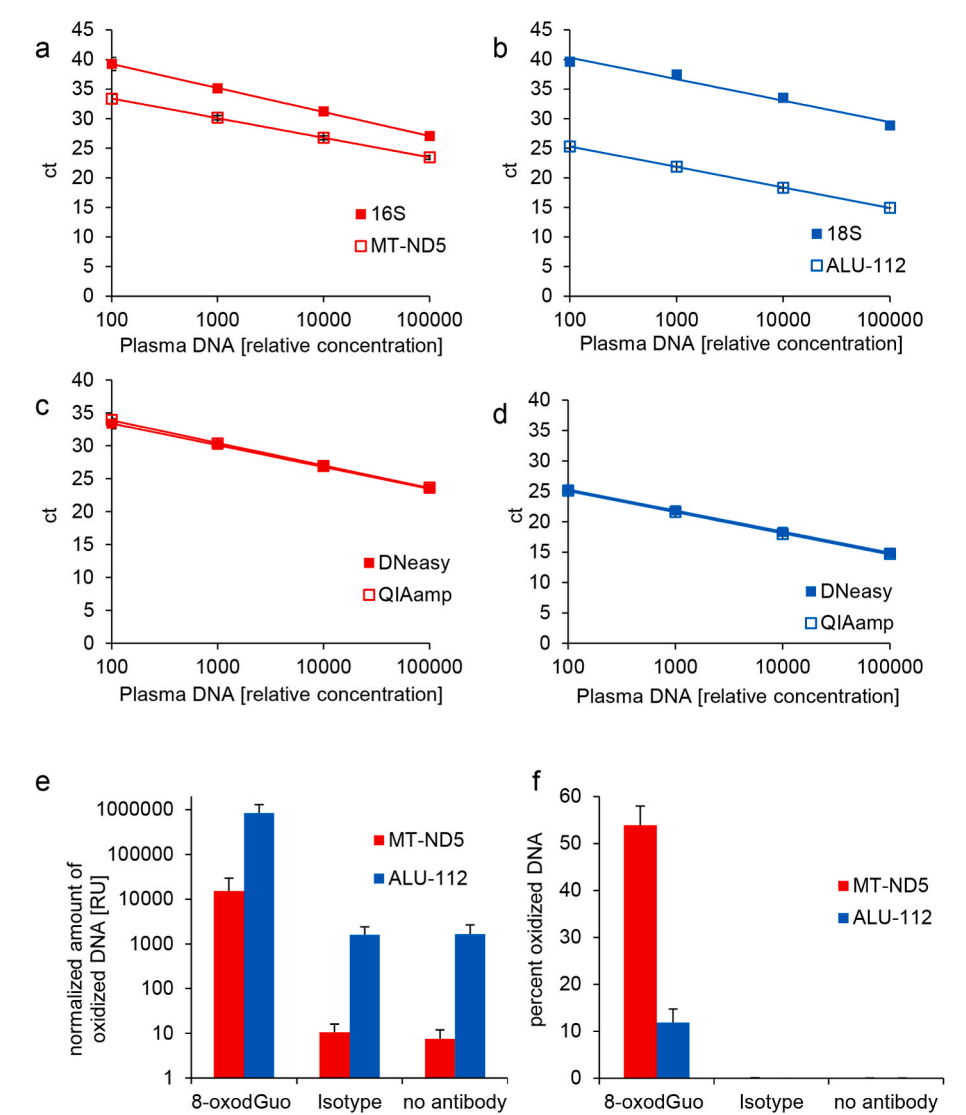


Fig. 2. Sensitive detection of nuclear and mitochondrial DNA from human plasma is facilitated by short qPCR amplicons and repetitive DNA elements. A-d) DNA was isolated from 190 µl citrated plasma and harvested in 30 µl buffer. Plasma DNA was subjected to serial 10-fold dilution and 2 µl of each dilution were applied in qPCR analysis. A relative plasma DNA concentration of 100 000 refers to undiluted plasma DNA. Mean \pm SD of biological replicates (n = 2) are depicted. Comparison of a) 50 nM 16S and 200 nM MT-ND5 primers, b) 50 nM 18S and 200 nM ALU-112 primers, c) DNeasy Blood & Tissue Kit (standard DNA isolation) and QIAamp DSP DNA Blood Mini Kit (proposed for improved shortfragment DNA isolation) in conjunction with 200 nM MT-ND5 primers, d) DNeasy Blood & Tissue Kit and QIAamp DSP DNA Blood Mini Kit in conjunction with 200 nM ALU-112 primers. Note that data points of the two DNA isolation variants overlap in c and d and that SDs are barely visible in a-d due to their small values. E) and f) Streptavidin coated microbeads were coupled with biotinylated antibodies against 8-oxodGuo, isotype control or were left uncoupled (no antibody). IP was performed according to the streptavidin-based protocol with DNA isolated from 190 μl of citrated plasma. Mean \pm SD represent biological replicates (n = 4). E) The normalized amount of oxidized DNA or f) the percent oxidized DNA is illustrated. Note that the y-axis in e) is depicted as a logarithmic scale. RU, relative units.

Table 1) with a target sequence of 55 bp and optimal primer efficiency around 2.0 for both, isolated plasma DNA and neutrophil DNA (Supplementary Tables 4 and 5). As mitochondrial DNA has also been integrated into the nuclear chromatin during evolution [49], primers targeting mitochondrial fragments may erroneously co-amplify nuclear sequences of mitochondrial origin (numts). We compared our selected MT-ND5 primer set to a number of primers reported to either exclusively detect mitochondrial DNA (HMTDNA, MT-ND1-1 and MT-ND5-1) or to co-amplify nuclear DNA fragments (MT-ND1-2 and MT-ND2) [50,51]. Signals from 143B.TK⁻ ρ^0 cells devoid of mitochondrial DNA were low with the MT-ND5 primer set and were comparable to other primers selectively detecting mitochondrial DNA but not numts (Supplementary Fig. 3).

Amplification of highly repetitive sequence stretches proved best for the detection of nuclear DNA. When target sequences in the COL1A1 promoter, TP53 promoter, LINE-1 ORF2 and *Alu* elements were assessed (Supplementary Table 1) the *ALU*-112 primer set with primer efficiency at 1.9 (Supplementary Tables 4 and 5) and amplicon length of 112 bp was highly sensitive in nuclear DNA detection and showed best specificity in terms of background signal and melting profile.

In a direct comparison of the 16S/MT-ND5 and 18S/ALU-112 primer sets with serial dilution of plasma DNA, the newly adapted primers outperformed the original 16S/18S set in primer efficiency as well as detection sensitivity of mitochondrial and nuclear DNA over a 1000-fold dilution range (Figs. 2a and b and Supplementary Table 5). Of note, samples containing <0.1% (v/v) of plasma DNA or samples without template (NTC) resulted in aberrant ALU-112 amplicons with a higher melting temperature, thus necessitating the inclusion of melting profiles in the analysis (Supplementary Fig. 4).

Sensitivity of mitochondrial or nuclear sequence detection could not be further enhanced by applying a specialized plasma DNA isolation method previously reported for improved recovery of short DNA fragments [48] (Figs. 2c and d).

Finally, we combined the established streptavidin-based IP procedure for oxidized DNA and the optimized qPCR detection of nuclear and mitochondrial DNA in the assessment of plasma samples from four distinct donors. The final protocol allowed for the specific detection of oxidized DNA (without unspecific binding to isotype control coated or uncoupled beads) and the discrimination of nuclear *versus* mitochondrial origin (Figs. 2e and f).

3.3. Non-oxidized nuclear DNA rather than oxidized mitochondrial DNA reflects increased NET formation in AAA patients

Since NET formation is a hallmark of AAA and is associated with the release of DNA, we aimed to compare the levels of oxidized mitochondrial and nuclear DNA to markers of neutrophil activation and NET formation in 39 AAA patients and 39 controls. The study cohorts were group-matched for age, sex and smoking status. The significantly higher prevalence of AAA in men compared to women [52] was reflected in the patient cohort (95%) and was matched by the controls (87%). The groups further showed a comparable frequency of co-morbidities such as PAD, stroke, myocardial infarction, diabetes mellitus and nephropathy (Tables 1 and 2). However, the cohorts presented significantly different with regard to hypertension, hyperlipidemia, coronary heart disease and chronic obstructive pulmonary disease (COPD). Of note, AAA patients and controls showed a comparable profile of routine blood parameters (including C-reactive protein) except for the established AAA marker D-dimer, which was highly elevated (Table 2).

IPs for oxidized DNA were performed in groups of 6 plasma samples (three AAA patients and three controls to minimize bias due to experimental variability). An internal calibrator was applied to each qPCR run and presented highly reproducible throughout the entire set of experiments: cT values of the internal calibrator for MT-ND5 and ALU-112 primer ranged at 22.88 \pm 0.04 and 14.06 \pm 0.05 (mean \pm SD, n = 13), respectively. Efficiencies for MT-ND5 and ALU-112 primers were

Table 1Patient and control demographics: categorical variables.

Characteristic	Control (N = 39)	AAA (N = 39)	P-value	
	N (%)	N (%)		
Sex				
Female	5 (12.8%)	2 (5.1%)	0.431	
Male	34 (87.2%)	37 (94.9%)		
Smoker status				
Never	9 (23.1%)	3 (7.7%)	0.077	
Past	18 (46.2%)	16 (41.0%)		
Current	12 (30.8%)	20 (51.3%)		
Hypertension	24 (61.5%)	33 (84.6%)	0.022	
Hyperlipidemia	12 (30.8%)	33 (84.6%)	< 0.001	
Peripheral artery disease	4 (10.3%)	7 (17.9%)	0.329	
Coronary heart disease	4 (10.3%)	14 (35.9%)	0.007	
Myocardial infarction	3 (7.7%)	9 (23.1%)	0.060	
Stroke	4 (10.3%)	2 (5.1%)	0.337	
Diabetes mellitus	4 (10.3%)	8 (20.5%)	0.209	
COPD	5 (12.8%)	14 (35.9%)	0.018	
Nephropathy/renal cysts	7 (17.9%)	12 (30.8%)	0.187	
Tumor or tumor treatment within the	2 (5.1%)	0 (0.0%)	0.247	
last year ^a				
Chronic inflammatory disease ^b	3 (7.7%)	0 (0.0%)	0.120	
Neurologic disorder ^c	1 (2.6%)	2 (5.1%)	0.500	
Autoimmune disease ^d	2 (5.1%)	1 (2.6%)	0.500	
Hematological disease ^e	0 (0.0%)	1 (2.6%)	0.500	
AAA family history				
No	35 (89.7%)	34 (87.2%)	0.602	
Yes	4 (10.3%)	4 (10.3%)		
Unknown	0 (0.0%)	1 (2.6%)		
AAA morphology				
Saccular		9 (23.1%)		
Fusiform		24 (61.5%)		
Excentric		2 (5.1%)		
Unknown		4 (10.3%)		
ILT presence				
No		1 (2.6%)		
Yes		35 (89.7%)		
Unknown		3 (7.7%)		

AAA, abdominal aortic aneurysm; COPD, chronic obstructive pulmonary disease; ILT, intraluminal thrombus. P-values according to Chi square or Fisher exact test are indicated. Please note that these patient and control cohorts have also been investigated in the context of other studies with respect to distinct explorative parameters [45,53,82].

- ^a Colorectal cancer, prostate cancer.
- ^b Rheumatoid arthritis, chronic hepatitis B, psoriasis.
- ^c Parkinson's disease, polyneuropathy.
- d Hashimoto's thyroiditis, psoriasis.
- ^e Monoclonal gammopathy of undetermined significance.

determined using the internal calibrator as 1.998 and 1.934, respectively, which is comparable to the values established with plasma DNA during the IP optimization process (see Supplementary Table 5). These efficiencies were applied for calculation of oxidized (8-oxodGuo positive) and non-oxidized (8-oxodGuo negative) mitochondrial and nuclear DNA content normalized to the internal calibrator.

Based on MT-ND5 detection, we observed borderline significance for elevated levels of oxidized mitochondrial DNA in plasma of AAA patients compared to controls (p = 0.053), whereas the amount of non-oxidized and total mitochondrial DNA did not differ. Of note, the proportion of oxidized to non-oxidized mitochondrial DNA was also comparable between groups (Fig. 3a–d, Supplementary Table 6). For nuclear DNA, the amount of circulating non-oxidized (p = 0.007) and total (p = 0.010) DNA presented significantly increased in AAA patients (Fig. 4a and c, Supplementary Table 6). In contrast, the amount of oxidized DNA was comparable between groups, resulting in a lower proportion of oxidized nuclear DNA in AAA patients than controls (p < 0.001, Fig. 4b and d, Supplementary Table 6). However, when the percentages of oxidized mitochondrial and nuclear DNA were set in relation, we observed significantly elevated values for AAA patients, which can be

.0

control

AAA

Table 2Patient and control demographics: metric variables.

Characteristic	Control (N = 39)	AAA (N = 39)	P-value
	Median (IQR)	Median (IQR)	
Age [years]	68.0 (13.3)	71.2 (10.7)	0.877
Body mass index [kg/m ²]	26.5 (5.5)	27.8 (5.5)	0.845
White blood cells [G/l]	5.70 (2.10)	6.40 (2.00)	0.092
Lymphocytes [G/l]	1.70 (0.70)	1.60 (1.00)	0.216
Monocytes [G/l]	0.50 (0.20)	0.50 (0.30)	0.896
Neutrophils [G/l]	3.60 (1.50)	3.90 (1.40)	0.182
Red blood cells [T/l]	4.72 (0.73)	4.57 (0.76)	0.287
Hemoglobin [g/dl]	14.20 (2.40)	14.60 (2.20)	0.675
Hematocrit [%]	42.00 (6.20)	41.50 (6.50)	0.996
Platelets [G/l]	174.00 (73.00)	155.00 (88.00)	0.143
C-reactive protein [mg/dl]	0.27 (0.47)	0.30 (0.39)	0.261
Fibrinogen - Clauss [mg/dl]	379.50 (102.00)	394.00 (129.00)	0.819
D-dimer [μg/ml]	0.48 (0.51)	1.27 (1.65)	< 0.001
Maximum AAA diameter [mm]		55.85 (11.25)	
Aneurysm volume [cm ³]		140.36 (79.63)	
Maximum ILT diameter [mm]		20.90 (10.40)	
ILT volume [cm ³]		74.69 (83.38)	

AAA, abdominal aortic aneurysm; ILT, intraluminal thrombus; IQR, interquartile range.

P-values according to Mann-Whitney *U* test are indicated. Please note that these patient and control cohorts have also been investigated in the context of other studies with respect to distinct explorative parameters [45,53,82].

translated into an enrichment of mitochondrial *versus* nuclear DNA within the oxidized DNA fraction in AAA patients (p < 0.001, Fig. 4e, Supplementary Table 6). Interestingly, amounts of circulating plasma mitochondrial and nuclear DNA did not correlate, regardless of their oxidation status (Supplementary Table 7).

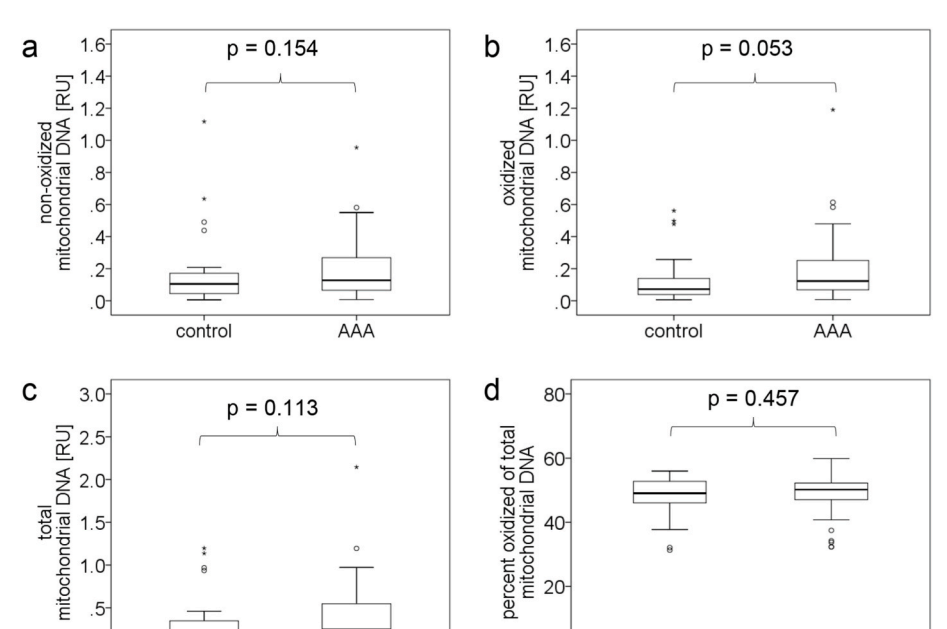
To test for potential confounders, we first conducted a univariable analysis by binary logistic regression for the investigated plasma DNA parameters as well as for patient co-morbidities and various other demographic variables (Supplementary Table 8). Parameters with a significance level <0.1 were entered in multivariable analysis. Of note, the percentage of oxidized nuclear DNA (Table 3) and the ratio of oxidized mitochondrial to nuclear DNA (Table 4) prevailed as independent predictors for the presence of AAA along with hyperlipidemia and COPD. Comparably, non-oxidized nuclear (Supplementary Table 9) and total

nuclear DNA (Supplementary Table 10) showed borderline significance with p-values of 0.051 and 0.054, respectively, while oxidized mitochondrial DNA had no independent diagnostic marker value (Supplementary Table 11).

We additionally assessed markers of neutrophil activation (NGAL, NE, MPO) and NET formation (DNA-histone complexes and citH3) and tested for association with the measured DNA parameters. As we have previously reported [45,53], plasma levels of MPO and citH3 were significantly elevated in AAA patients compared to controls, whereas NGAL, NE and DNA-histone complexes were equally distributed between the investigated groups in this study (Supplementary Table 6). MPO as well as citH3 significantly and strongly correlated with nuclear DNA, regardless of its oxidation status (Fig. 5, Supplementary Table 7). For mitochondrial DNA, we observed a low but significant correlation with MPO independent of the DNA oxidation status whereas circulating citH3 showed no association with mitochondrial DNA (Supplementary Table 7).

4. Discussion

In this study, we established a protocol for the analysis of oxidized (8-oxodGuo positive) DNA from human plasma samples applicable for the discrimination between mitochondrial and nuclear origin. In the optimized procedure, DNA was first isolated from plasma, was then subjected to streptavidin-based IP with biotinylated antibodies targeting 8-oxodGuo and subsequently analyzed by qPCR with primers covering mitochondrial (MT-ND5) or nuclear (ALU-112) DNA elements. Importantly, immediate immunoprecipitation of oxidized DNA from crude plasma failed, i.e. lacked specificity. The initial protein G based IP approach proved not advisable, as the interaction between protein G and the target antibody is reversible and likely replaced by the about 400fold excess of immunoglobulin G in human plasma. Similarly, plasma biotin may interfere with antibody-coupled biotin in binding to streptavidin-coated microbeads and sample dilution cannot resolve the issue, since 10% (v/v) of plasma was found sufficient to abrogate assay specificity. Instead, isolation of plasma DNA prior to IP presented as an option to circumvent these complications, provided that the isolation process per se does not modify the DNA oxidation status. It has previously been demonstrated that - depending on the sample matrix and



0-

Fig. 3. The oxidized fraction of mitochondrial DNA shows a trend for higher levels in plasma of AAA patients. A-d) DNA was isolated from plasma, processed according to the streptavidin-based IP protocol and the mitochondrial DNA content relative to the calibrator was quantified by qPCR analysis with primers targeting MT-ND5. The normalized amounts of a) non-oxidized and b) oxidized as well as c) total mitochondrial DNA and d) percent oxidized of total mitochondrial DNA are illustrated. Boxplots and p-values according to Mann-Whitney U test are indicated (n = 39 per group). RU, relative units.

AAA

control

0

control

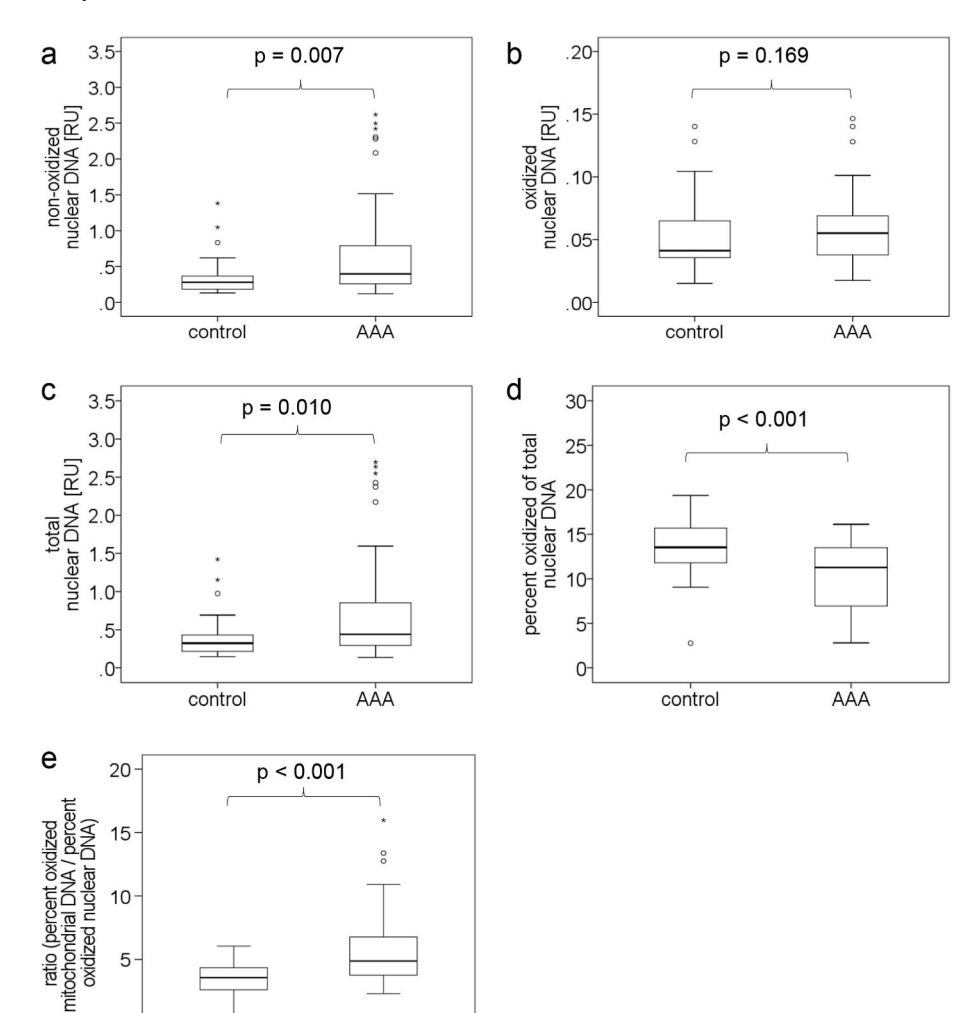


Fig. 4. The amounts of non-oxidized and total nuclear DNA are significantly elevated in plasma of AAA patients. A-e) DNA was isolated from plasma, processed according to the streptavidin-based IP protocol and the nuclear DNA content relative to the calibrator was quantified by qPCR analysis with primers targeting ALU-112. The normalized amounts of a) non-oxidized and b) oxidized as well as c) total nuclear DNA and d) the percent oxidized of total nuclear DNA are illustrated. E) A ratio (compare Methods) was calculated to set the oxidized mitochondrial and nuclear DNA fractions into relation. Boxplots and p-values according to Mann-Whitney U test are indicated (n = 39 per group). RU, relative units.

 $\label{eq:table 3} \begin{tabular}{l}{l}{Multivariable analysis (binary logistic regression, method Enter) of AAA presence including the percentage of oxidized nuclear DNA and co-morbidities with $p < 0.1$ as listed in Supplementary Table 8.} \end{tabular}$

AAA

Parameter	p- value	Exp (B)	95% CI Lower value	95% CI Upper value
Percent oxidized of total nuclear DNA	0.007	0.763	0.628	0.927
Ever smoked	0.084	4.937	0.806	30.25
Hypertension	0.439	1.978	0.351	11.15
Hyperlipidemia	0.003	8.660	2.087	35.94
Coronary heart disease	0.281	4.259	0.305	59.47
Myocardial infarction	0.318	0.215	0.011	4.387
COPD	0.038	4.775	1.089	20.94
Constant	0.787	0.638		

CI, confidence interval; COPD, chronic obstructive pulmonary disease; DNA, deoxyribonucleic acid; Exp(B), odds ratio.

DNA isolation method – the extent of DNA-incorporated 8-oxodGuo may be substantially increased [22]. In our protocol, we avoided critical steps of DNA manipulation known to generate artificially high levels of 8-oxodGuo such as the application of phenol, lengthy proteinase K digestion and air-drying of DNA [54–56]. Various measures have been suggested to diminish adventitious DNA oxidation during extraction from cells such as the pre-isolation of nuclei, the addition of desferrioxamine or 2,2,6,6-tetramethylpiperidine-N-oxyl to extraction buffers and the application of sodium iodide for DNA precipitation [57,58].

Table 4 Multivariable analysis (binary logistic regression, method Enter) of AAA presence including the ratio of oxidized mitochondrial to nuclear DNA and comorbidities with p < 0.1 as listed in Supplementary Table 8.

Parameter	p-value	Exp (B)	95% CI Lower value	95% CI Upper value
Ratio of oxidized mitochondrial to nuclear	0.011	2.094	1.186	3.697
DNA				
Ever smoked	0.088	4.925	0.790	30.70
Hypertension	0.305	2.445	0.444	13.47
Hyperlipidemia	0.014	5.956	1.432	24.77
Coronary heart disease	0.230	5.025	0.359	70.30
Myocardial infarction	0.237	0.157	0.007	3.370
COPD	0.040	4.798	1.073	21.45
Constant	< 0.001	0.001		

CI, confidence interval; COPD, chronic obstructive pulmonary disease; DNA, deoxyribonucleic acid; Exp(B), odds ratio.

Furthermore, isolation of at least 30–50 μg DNA was recommended to minimize spurious DNA oxidation [27,59]. In comparison, plasma DNA is very dilute but does not necessitate harsh extraction methods, i.e. circulating cell-free DNA is retrieved by a rapid column-based technique, immediately followed by the immunoprecipitation step. In addition, the IP buffer may influence the DNA oxidation status: Cell culture media components – in contrast to PBS – can form ROS, in particular in the presence of light [60]. However, in our set of

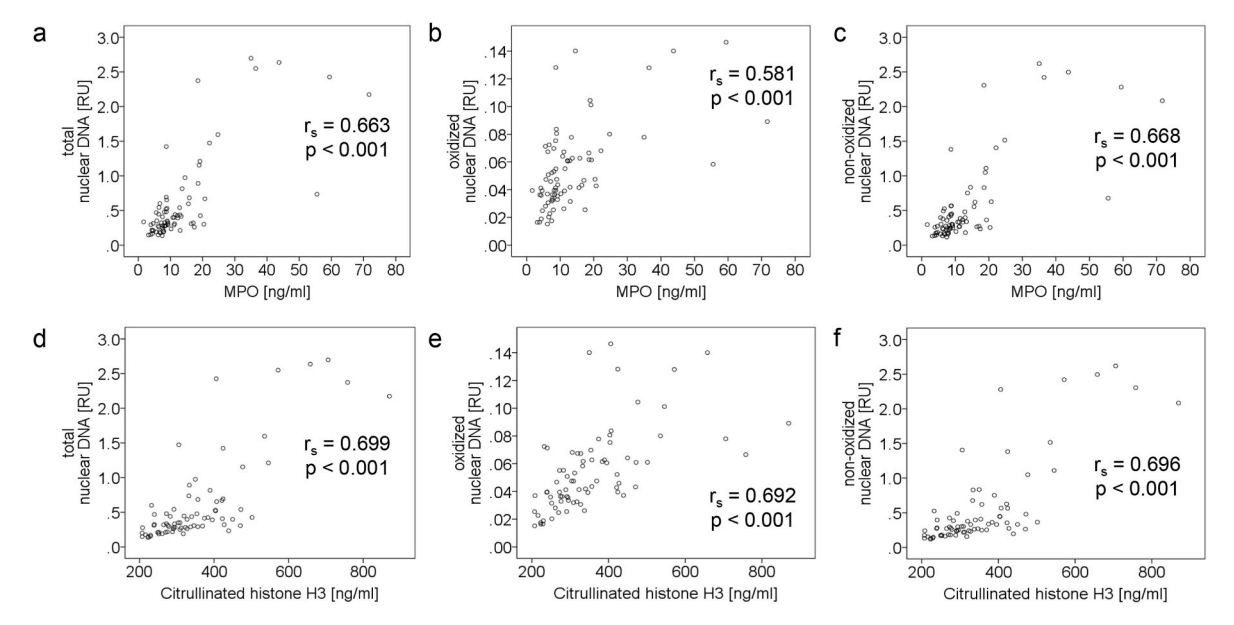


Fig. 5. Plasma MPO and citH3 correlate with nuclear DNA irrespective of oxidation status. DNA was isolated from plasma, processed according to the streptavidin-based IP protocol and the nuclear DNA content was quantified by qPCR analysis with primers targeting ALU-112. MPO and citH3 were assessed by ELISA. Correlations between MPO and a) total nuclear DNA, b) oxidized nuclear DNA or c) non-oxidized nuclear DNA as well as between citH3 and d) total nuclear DNA, e) oxidized nuclear DNA or f) non-oxidized nuclear DNA are visualized by scatterplots and expressed by Spearman's coefficients r_s and p-values (n = 77 for MPO, n = 76 for citH3). RU, relative units.

experiments, the applied IP buffer had a minor impact on the 8-oxodGuo content and mitochondrial DNA even demonstrated the lowest amount of oxidation after IP in RPMI 1640 medium. Importantly, by spiking partially oxidized DNA into plasma samples, we confirmed that the plasma matrix and the DNA isolation process had little influence on the DNA oxidation status. Thus, we concluded that DNA isolation from plasma serves to circumvent the detrimental effect of the plasma matrix on the IP process without artificially increasing the 8-oxodGuo content. The optimized IP protocol was confirmed with plasma from four donors and showed negligible unspecific DNA binding to isotype control coated or uncoupled beads.

Compared to a previously published protocol [17], we further increased the sensitivity of qPCR-based detection of circulating mitochondrial and nuclear DNA by decreasing the amplicon length and by targeting highly repetitive nuclear DNA sequences as previously suggested [61]. The initially applied 16S and 18S primer pairs proved suboptimal as they covered rather large sequence stretches (103 bp and 151 bp, respectively) when compared to plasma cell-free DNA fragments: The predominant portion of circulating nuclear DNA ranges between 130 and 200 bp (peaking at 166-167 bp) and plasma mitochondrial DNA was reported to be even smaller, peaking at 42 bp, 90 bp or 140 bp, depending on the applied detection method [47,48]. Thus, qPCR sensitivity for mitochondrial and nuclear DNA could be improved by application of the selected MT-ND5 and ALU-112 primers, which also exhibited primer efficiencies superior to the initial 16S and 18S primer sets. When titrating the starting material, i.e. the isolated plasma DNA by 1:1000, the specific signal and NTC background for ALU-112 were set apart by about 8 qPCR cycles, which translates to a maximum of 0.4% of background noise adding to the specific plasma DNA signal. Furthermore, the unspecific reactions yield qPCR products with aberrant melting profile, i.e. can be easily detected. Of note, background signals upon amplification of ALU sequences are common and were suggested to be inherent to qPCR components rather than an air-borne, user- or equipment-derived contamination [61-63]. With regard to mitochondrial DNA, "unspecific" signals could potentially arise from primer sets erroneously co-amplifying numts. When we tested the chosen MT-ND5 primer pair with DNA isolated from 143B.TKρ⁰ cells (lacking mitochondrial DNA) versus parental 143B.TK⁻ cells we found that signal interference from numts was low and comparable to primer sets reportedly being highly specific for mitochondrial sequences.

Standard chromatography methods detect oxidative DNA alterations on a nucleobase level. Thus, assessment of base lesions within DNA strands requires the breakdown of DNA into single bases by acid or enzyme [23,64]. With these methods, it is not possible to trace circulating cell-free oxidative DNA modifications to a nuclear or mitochondrial origin. We thus adopted an antibody-based IP step to first separate oxidized from non-oxidized DNA fragments and then applied qPCR to allocate these fragments to their subcellular source. Of note, concerns have been raised regarding the applicability of immunological methods for the detection of oxidized DNA as the reported antibodies may exhibit cross-reactivity with the parental or other modified bases at the expense of assay specificity [2,3]. With regard to the clone applied in this work (15A3), apart from 8-oxodGuo, the antibody also recognizes 8-oxoGua (the oxidized free base) and 8-oxoGuo (the oxidized RNA-incorporated base) [44], thus potentially occupying binding capacities during IP. However, by the preceding DNA isolation, the oxidized free base is efficiently removed and in the subsequent qPCR step, RNA molecules are not amplified, hence not contributing to the obtained signal. Binding affinities of 15A3 to 8-oxodGuo versus the parental 2'-deoxyguanosine (dGuo) are in the range of roughly 7000:1 [44], which also argues for a very low probability of IP "contamination" by non-oxidized plasma DNA fragments.

The determined percentages of oxidized nuclear (median 12.6%) and mitochondrial (median: 49.4%) plasma DNA may appear high, since human tissue levels of 8-oxodGuo were quantified in the range of approximately 1–1000 lesions per 10⁶ dGuo, depending on the studied tissue and applied method [22,65,66]. Since plasma serves as a pool collecting DNA from cells undergoing apoptosis, necrosis or NET formation, it is likely to be enriched in damaged molecules. In addition, 8-oxodGuo is not generated or degraded in circulation in substantial amounts [67], further suggesting that the determined plasma levels of oxidized DNA are reflecting tissue sites of cell destruction and release of modified DNA.

There are a few reports introducing other techniques for the detection of 8-oxodGuo bearing DNA and the attribution to a nuclear or

mitochondrial origin. Lin *et al.* subjected isolated tissue or leukocyte DNA to digestion with 8-oxoguanine glycosylase, thus removing 8-oxoGua which decreases amplification efficiency in subsequent qPCR analysis. The Δ ct difference between digested and untreated DNA served as measure for the amount of oxidative DNA damage [68,69]. Another method utilized "chemical tagging", i.e. customized probes targeting 8-oxodGuo to pull down oxidized DNA for qPCR analysis [70]. In contrast to our antibody-based approach, these probes are not readily available. Additionally, both methods have not been applied to plasma samples and it remains to be elucidated whether they would be suitable for the direct analysis of plasma compared to isolated DNA.

Finally, we applied our optimized protocol for the concomitant assessment of oxidized nuclear and mitochondrial DNA to compare plasma levels in AAA patients and healthy (non-AAA) controls. While non-oxidized and total nuclear DNA was significantly elevated in circulation of aneurysm patients, levels of non-oxidized or total mitochondrial DNA did not differ between groups. Yet, there was a trend for increased plasma concentrations of oxidized mitochondrial DNA in the AAA group, and we found a higher proportion of plasma mitochondrial DNA to be oxidized compared to nuclear DNA. In line with previous reports, the elevated level of oxidized mitochondrial DNA would be considered a pro-inflammatory driver of chronic disease [17]. Of note, plasma levels of mitochondrial and nuclear DNA did not correlate, irrespective of their oxidation status, probably indicating their differential release or clearance from circulation. Similarly, a correlation of circulating mitochondrial and nuclear DNA was absent in a cohort of patients with prostate cancer and benign disease [71]. However, plasma levels of nuclear (but not mitochondrial) DNA correlated strongly with markers of neutrophil activation and NET formation in our study, which indicates that the majority of circulating nuclear DNA likely emanates from sites of inflammatory cell destruction such as the aneurysmatic lesion.

The study groups were matched for three variables known to affect oxidized or mitochondrial DNA levels (age [72-74], sex [72,75] and smoking habit [76,77]) and were equally distributed for co-morbidities reported to be associated with 8-oxodGuo levels such as PAD [5], stroke [78] and diabetes mellitus [79,80]. However, they presented significantly different with regard to other conditions that may shape the circulating profile of oxidized DNA like hypertension, hyperlipidemia, coronary heart disease and COPD. Multivariable analysis revealed that the percentage of oxidized nuclear DNA and the ratio between percent oxidized mitochondrial to nuclear DNA (along with hyperlipidemia and COPD) were independent predictors of AAA presence. It should be emphasized that it was indeed the circulating, non-oxidized nuclear DNA that was highly increased in aneurysm patients, thus resulting in a lower proportion of oxidized nuclear DNA and a predominance of oxidized mitochondrial versus nuclear DNA fraction. These relative scores proved to be more sensitive in multivariable analysis to discriminate between AAA patients and healthy controls than the measured amount of non-oxidized (or total) nuclear DNA. Yet, the latter reached borderline significance in this explorative setting and would certainly constitute the more readily assessable parameter, i.e. should also be included in a further validation study with a larger patient and control collective.

Although the proposed protocol proved highly sensitive and specific, some limitations must be taken into account. First, since primers for amplification of nuclear DNA target repetitive sequences (*Alu* elements cover approximately 10% of the human genome [81]) as opposed to primers targeting mitochondrial DNA, the calculated amounts of circulating nuclear and mitochondrial DNA cannot be set into relation and thus do not reflect their actual *in vivo* proportion. Second, based on the assumption that oxidized DNA binds to the IP antibody irrespective of the quantity of incorporated 8-oxodGuo, this technique gives no information regarding the degree of oxidation of individual DNA stretches. Third, the data do not provide information regarding the cellular source of plasma DNA. Although correlations with other blood parameters may

offer indications, they are no proof for a causal relation. Fourth, while spiking of partially oxidized DNA into plasma samples indicated little changes during sample preparation, we cannot exclude spurious DNA oxidation by the established procedure. Yet, the high degree of DNA oxidation recorded for circulating, cell-free DNA in plasma might explain a lower impact of oxidation artefacts introduced during *in vitro* manipulation.

5. Conclusions

In summary, the developed method is suited for biomarker applications, i.e. to relatively compare oxidized circulating cell-free DNA between patient groups or in longitudinal patient monitoring. The protocol enables researchers to quantitate levels of circulating oxidized DNA in human plasma samples (in relation to calibrators or controls) and to determine the nuclear or mitochondrial origin. Since mitochondrial DNA and oxidized DNA species exhibit pro-inflammatory features, while nuclear DNA predominantly reflects cell death and tissue destruction, the differential assessment of circulating DNA species and their oxidation status provides more detailed information and a tool to monitor disease burden and activity.

Data availability

The data used to support the findings of this study are available from the corresponding author upon request.

Declarations of competing interest (for all authors)

None.

Funding statement

This work was primarily supported by the Austrian Science Fund [SFB subproject F 5409-B21 issued to CB]. Viktoria Knöbl is personally supported by the DocFund doctoral program [DOC 59-833] of the Austrian Science Fund. The funders had no role in study design, data collection, data analysis, data interpretation, decision to publish or preparation of the manuscript.

Acknowledgement

The graphical abstract was created with BioRender.com.

Appendix A. Supplementary data

Supplementary data to this article can be found online at https://doi. org/10.1016/j.freeradbiomed.2023.06.014.

Abbreviations

16S MT-RNR2/mitochondrially encoded 16S ribosomal RNA

18S RNA18S5/18S ribosomal RNA 5

8-oxodGuo 8-oxo-7,8-dihydro-2'-deoxyguanosine

 $\begin{array}{lll} \text{8-oxoGua} & \text{8-oxo-7,8-dihydroguanine} \\ \text{8-oxoGuo} & \text{8-oxo-7,8-dihydroguanosine} \\ \rho^0 & \text{mitochondrial DNA-less} \end{array}$

AAA abdominal aortic aneurysm

ALU ALU element

BMI body mass index

CAD coronary artery disease

CI confidence interval

citH3 citrullinated histone H3

COPD chronic obstructive pulmonary disease

ct cycle threshold dGuo 2'-deoxyguanosine

DNA deoxyribonucleic acid

ELISA enzyme-linked immunosorbent assay

Exp(B) odds ratio

HPLC high performance liquid chromatography

IFN-α interferon alpha
 ILT intraluminal thrombus
 IP immunoprecipitation
 IQR interquartile range
 MPO myeloperoxidase
 MS mass spectrometry

MS/MS tandem mass spectrometry

MT-ND5 mitochondrially encoded NADH:ubiquinone oxidoreductase

core subunit 5 NE neutrophil elastase

NET neutrophil extracellular trap

NGAL neutrophil gelatinase-associated lipocalin

NFW nuclease free water NTC no template control

numts nuclear sequences of mitochondrial origin

PAD peripheral artery disease PBS phosphate buffered saline

qPCR quantitative polymerase chain reaction

 R^2 regression coefficient ROS reactive oxygen species r_s Spearman's coefficient

RU relative units

SLE systemic lupus erythematosus TK thymidine kinase-negative

References

- [1] J. Cadet, K.J.A. Davies, Oxidative DNA damage & repair: an introduction, Free Radic. Biol. Med. 107 (2017) 2–12.
- [2] J. Cadet, K.J.A. Davies, M.H. Medeiros, P. Di Mascio, J.R. Wagner, Formation and repair of oxidatively generated damage in cellular DNA, Free Radic. Biol. Med. 107 (2017) 13–34.
- [3] H.E. Poulsen, L.L. Nadal, K. Broedbaek, P.E. Nielsen, A. Weimann, Detection and interpretation of 8-oxodG and 8-oxoGua in urine, plasma and cerebrospinal fluid, Biochim. Biophys. Acta 1840 (2) (2014) 801–808.
- [4] K.C. Cheng, D.S. Cahill, H. Kasai, S. Nishimura, L.A. Loeb, 8-Hydroxyguanine, an abundant form of oxidative DNA damage, causes G——T and A——C substitutions, J. Biol. Chem. 267 (1) (1992) 166–172.
- [5] L. Loffredo, P. Pignatelli, R. Cangemi, P. Andreozzi, M.A. Panico, V. Meloni, F. Violi, Imbalance between nitric oxide generation and oxidative stress in patients with peripheral arterial disease: effect of an antioxidant treatment, J. Vasc. Surg. 44 (3) (2006) 525–530.
- [6] F. Xiang, X. Shuanglun, W. Jingfeng, N. Ruqiong, Z. Yuan, L. Yongqing, Z. Jun, Association of serum 8-hydroxy-2'-deoxyguanosine levels with the presence and severity of coronary artery disease, Coron. Artery Dis. 22 (4) (2011) 223–227.
- [7] A. Di Minno, L. Turnu, B. Porro, I. Squellerio, V. Cavalca, E. Tremoli, M.N. Di Minno, 8-Hydroxy-2-Deoxyguanosine levels and cardiovascular disease: a systematic review and meta-analysis of the literature, Antioxid. Redox Signal. 24 (10) (2016) 548–555.
- [8] P. Atukeren, B. Yavuz, H.O. Soydinc, S. Purisa, H. Camlica, M.K. Gumustas, I. Balcioglu, Variations in systemic biomarkers of oxidative/nitrosative stress and DNA damage before and during the consequent two cycles of chemotherapy in breast cancer patients, Clin. Chem. Lab. Med. 48 (10) (2010) 1487–1495.
- [9] Y. Ma, L. Zhang, S. Rong, H. Qu, Y. Zhang, D. Chang, H. Pan, W. Wang, Relation between gastric cancer and protein oxidation, DNA damage, and lipid peroxidation, Oxid. Med. Cell. Longev. 2013 (2013), 543760.
- [10] A. Sliwinska, D. Kwiatkowski, P. Czarny, M. Toma, P. Wigner, J. Drzewoski, K. Fabianowska-Majewska, J. Szemraj, M. Maes, P. Galecki, T. Sliwinski, The levels of 7,8-dihydrodeoxyguanosine (8-oxoG) and 8-oxoguanine DNA glycosylase 1 (OGG1) a potential diagnostic biomarkers of Alzheimer's disease, J. Neurol. Sci. 368 (2016) 155–159.
- [11] H.T. Lee, C.S. Lin, C.S. Lee, C.Y. Tsai, Y.H. Wei, The role of hOGG1 C1245G polymorphism in the susceptibility to lupus nephritis and modulation of the plasma 8-OHdG in patients with systemic lupus erythematosus, Int. J. Mol. Sci. 16 (2) (2015) 3757–3768.
- [12] D. Villano, C. Vilaplana, S. Medina, R. Cejuela-Anta, J.M. Martinez-Sanz, P. Gil, H. G. Genieser, F. Ferreres, A. Gil-Izquierdo, Effect of elite physical exercise by triathletes on seven catabolites of DNA oxidation, Free Radic. Res. 49 (8) (2015) 973–983
- [13] S. Jahr, H. Hentze, S. Englisch, D. Hardt, F.O. Fackelmayer, R.D. Hesch, R. Knippers, DNA fragments in the blood plasma of cancer patients: quantitations and evidence for their origin from apoptotic and necrotic cells, Cancer Res. 61 (4) (2001) 1659–1665.

- [14] L. Jiang, S. Paone, S. Caruso, G.K. Atkin-Smith, T.K. Phan, M.D. Hulett, I.K.H. Poon, Determining the contents and cell origins of apoptotic bodies by flow cytometry, Sci. Rep. 7 (1) (2017), 14444.
- [15] B.K. Thakur, H. Zhang, A. Becker, I. Matei, Y. Huang, B. Costa-Silva, Y. Zheng, A. Hoshino, H. Brazier, J. Xiang, C. Williams, R. Rodriguez-Barrueco, J.M. Silva, W. Zhang, S. Hearn, O. Elemento, N. Paknejad, K. Manova-Todorova, K. Welte, J. Bromberg, H. Peinado, D. Lyden, Double-stranded DNA in exosomes: a novel biomarker in cancer detection, Cell Res. 24 (6) (2014) 766–769.
- [16] V. Brinkmann, U. Reichard, C. Goosmann, B. Fauler, Y. Uhlemann, D.S. Weiss, Y. Weinrauch, A. Zychlinsky, Neutrophil extracellular traps kill bacteria, Science (New York, N.Y.) 303 (5663) (2004) 1532–1535.
- [17] C. Lood, L.P. Blanco, M.M. Purmalek, C. Carmona-Rivera, S.S. De Ravin, C. K. Smith, H.L. Malech, J.A. Ledbetter, K.B. Elkon, M.J. Kaplan, Neutrophil extracellular traps enriched in oxidized mitochondrial DNA are interferogenic and contribute to lupus-like disease, Nat. Med. 22 (2) (2016) 146–153.
- [18] W. Stoiber, A. Obermayer, P. Steinbacher, W.D. Krautgartner, The role of reactive oxygen species (ROS) in the formation of extracellular traps (ETs) in humans, Biomolecules 5 (2) (2015) 702–723.
- [19] S. Yousefi, C. Mihalache, E. Kozlowski, I. Schmid, H.U. Simon, Viable neutrophils release mitochondrial DNA to form neutrophil extracellular traps, Cell Death Differ. 16 (11) (2009) 1438–1444.
- [20] L.V. Collins, S. Hajizadeh, E. Holme, I.M. Jonsson, A. Tarkowski, Endogenously oxidized mitochondrial DNA induces in vivo and in vitro inflammatory responses, J. Leukoc. Biol. 75 (6) (2004) 995–1000.
- [21] N. Dabrowska, A. Wiczkowski, Analytics of oxidative stress markers in the early diagnosis of oxygen DNA damage, Adv. Clin. Exp. Med. 26 (1) (2017) 155–166.
- [22] M.L. Hamilton, Z. Guo, C.D. Fuller, H. Van Remmen, W.F. Ward, S.N. Austad, D. A. Troyer, I. Thompson, A. Richardson, A reliable assessment of 8-oxo-2-deoxyguanosine levels in nuclear and mitochondrial DNA using the sodium iodide method to isolate DNA, Nucleic Acids Res. 29 (10) (2001) 2117–2126.
- [23] R. Amouroux, B. Nashun, K. Shirane, S. Nakagawa, P.W. Hill, Z. D'Souza, M. Nakayama, M. Matsuda, A. Turp, E. Ndjetehe, V. Encheva, N.R. Kudo, H. Koseki, H. Sasaki, P. Hajkova, De novo DNA methylation drives 5hmC accumulation in mouse zygotes, Nat. Cell Biol. 18 (2) (2016) 225–233.
- [24] N.R. Gassman, E. Coskun, D.F. Stefanick, J.K. Horton, P. Jaruga, M. Dizdaroglu, S. H. Wilson, Bisphenol a promotes cell survival following oxidative DNA damage in mouse fibroblasts, PLoS One 10 (2) (2015), e0118819.
- [25] C.C. Smith, M.R. O'Donovan, E.A. Martin, hOGG1 recognizes oxidative damage using the comet assay with greater specificity than FPG or ENDOIII, Mutagenesis 21 (3) (2006) 185–190.
- [26] European Standards Committee on Oxidative DNA Damage (ESCODD), Measurement of DNA oxidation in human cells by chromatographic and enzymic methods, Free Radic. Biol. Med. 34 (8) (2003) 1089–1099.
- [27] A.R. Collins, J. Cadet, L. Möller, H.E. Poulsen, J. Viña, Are we sure we know how to measure 8-oxo-7,8-dihydroguanine in DNA from human cells? Arch. Biochem. Biophys. 423 (1) (2004) 57–65.
- [28] C.M. Gedik, A. Collins, Establishing the background level of base oxidation in human lymphocyte DNA: results of an interlaboratory validation study, Faseb. J. 19 (1) (2005) 82–84.
- [29] L.M. van der Waals, J.M.J. Jongen, S.G. Elias, K. Veremiyenko, K. Trumpi, A. Trinh, J. Laoukili, I. Ubink, S.J. Schenning-van Schelven, P.J. van Diest, I.H.M. Borel Rinkes, O. Kranenburg, Increased levels of oxidative damage in liver metastases compared with corresponding primary colorectal tumors: association with molecular subtype and prior treatment, Am. J. Pathol. 188 (10) (2018) 2369–2377.
- [30] L. Barregard, P. Moller, T. Henriksen, V. Mistry, G. Koppen, P. Rossner Jr., R. J. Sram, A. Weimann, H.E. Poulsen, R. Nataf, R. Andreoli, P. Manini, T. Marczylo, P. Lam, M.D. Evans, H. Kasai, K. Kawai, Y.S. Li, K. Sakai, R. Singh, F. Teichert, P. B. Farmer, R. Rozalski, D. Gackowski, A. Siomek, G.T. Saez, C. Cerda, K. Broberg, C. Lindh, M.B. Hossain, S. Haghdoost, C.W. Hu, M.R. Chao, K.Y. Wu, H. Orhan, N. Senduran, R.J. Smith, R.M. Santella, Y. Su, C. Cortez, S. Yeh, R. Olinski, S. Loft, M.S. Cooke, Human and methodological sources of variability in the measurement of urinary 8-oxo-7,8-dihydro-2'-deoxyguanosine, Antioxid. Redox Signal. 18 (18) (2013) 2377–2391.
- [31] N. Gehrke, C. Mertens, T. Zillinger, J. Wenzel, T. Bald, S. Zahn, T. Tuting, G. Hartmann, W. Barchet, Oxidative damage of DNA confers resistance to cytosolic nuclease TREX1 degradation and potentiates STING-dependent immune sensing, Immunity 39 (3) (2013) 482–495.
- [32] H. Wang, T. Li, S. Chen, Y. Gu, S. Ye, Neutrophil extracellular trap mitochondrial DNA and its autoantibody in systemic lupus erythematosus and a proof-of-concept trial of metformin, Arthritis Rheumatol. 67 (12) (2015) 3190–3200.
- [33] J. Klopf, C. Brostjan, W. Eilenberg, C. Neumayer, Neutrophil extracellular traps and their implications in cardiovascular and inflammatory disease, Int. J. Mol. Sci. 22 (2) (2021).
- [34] A. Warnatsch, M. Ioannou, Q. Wang, V. Papayannopoulos, Inflammation. Neutrophil extracellular traps license macrophages for cytokine production in atherosclerosis, Science (New York, N.Y.) 349 (6245) (2015) 316–320.
- [35] T.A. Fuchs, A. Brill, D. Duerschmied, D. Schatzberg, M. Monestier, D.D. Myers Jr., S.K. Wrobleski, T.W. Wakefield, J.H. Hartwig, D.D. Wagner, Extracellular DNA traps promote thrombosis, Proc. Natl. Acad. Sci. U. S. A. 107 (36) (2010) 15880–15885.
- [36] S. Delbosc, J.M. Alsac, C. Journe, L. Louedec, Y. Castier, M. Bonnaure-Mallet, R. Ruimy, P. Rossignol, P. Bouchard, J.B. Michel, O. Meilhac, Porphyromonas gingivalis participates in pathogenesis of human abdominal aortic aneurysm by neutrophil activation. Proof of concept in rats, PLoS One 6 (4) (2011), e18679.
- [37] A.K. Meher, M. Spinosa, J.P. Davis, N. Pope, V.E. Laubach, G. Su, V. Serbulea, N. Leitinger, G. Ailawadi, G.R. Upchurch Jr., Novel role of IL (Interleukin)-1beta in

- neutrophil extracellular trap formation and abdominal aortic aneurysms, Arterioscler. Thromb. Vasc. Biol. 38 (4) (2018) 843–853.
- [38] M. Wei, X. Wang, Y. Song, D. Zhu, D. Qi, S. Jiao, G. Xie, Y. Liu, B. Yu, J. Du, Y. Wang, A. Qu, Inhibition of peptidyl arginine deiminase 4-dependent neutrophil extracellular trap formation reduces angiotensin II-induced abdominal aortic aneurysm rupture in mice, Frontiers Cardiovasc. Med. 8 (2021), 676612.
- [39] H. Yan, H.F. Zhou, A. Akk, Y. Hu, L.E. Springer, T.L. Ennis, C.T.N. Pham, Neutrophil proteases promote experimental abdominal aortic aneurysm via extracellular trap release and plasmacytoid dendritic cell activation, Arterioscler. Thromb. Vasc. Biol. 36 (8) (2016) 1660–1669.
- [40] S. Yang, L. Chen, Z. Wang, J. Chen, Q. Ni, X. Guo, W. Liu, L. Lv, G. Xue, Neutrophil extracellular traps induce abdominal aortic aneurysm formation by promoting the synthetic and proinflammatory smooth muscle cell phenotype via Hippo-YAP pathway, Transl. Res. 255 (2023) 85–96.
- [41] D. Costa, A.P. Marques, R.L. Reis, J.L. Lima, E. Fernandes, Inhibition of human neutrophil oxidative burst by pyrazolone derivatives, Free Radic. Biol. Med. 40 (4) (2006) 632–640.
- [42] H. Hayden, N. Ibrahim, J. Klopf, B. Zagrapan, L.M. Mauracher, L. Hell, T. M. Hofbauer, A.S. Ondracek, C. Schoergenhofer, B. Jilma, I.M. Lang, I. Pabinger, W. Eilenberg, C. Neumayer, C. Brostjan, ELISA detection of MPO-DNA complexes in human plasma is error-prone and yields limited information on neutrophil extracellular traps formed in vivo, PLoS One 16 (4) (2021), e0250265.
- [43] M.P. King, G. Attardi, Human cells lacking mtDNA: repopulation with exogenous mitochondria by complementation, Science (New York, N.Y.) 246 (4929) (1989) 500–503.
- [44] E.M. Park, M.K. Shigenaga, P. Degan, T.S. Korn, J.W. Kitzler, C.M. Wehr, P. Kolachana, B.N. Ames, Assay of excised oxidative DNA lesions: isolation of 8oxoguanine and its nucleoside derivatives from biological fluids with a monoclonal antibody column, Proc. Natl. Acad. Sci. U. S. A. 89 (8) (1992) 3375–3379.
- [45] W. Eilenberg, B. Zagrapan, S. Bleichert, N. Ibrahim, V. Knöbl, A. Brandau, L. Martelanz, M.T. Grasl, H. Hayden, P. Nawrozi, R. Rajic, C. Häusler, A. Potolidis, N. Schirwani, A. Scheuba, J. Klopf, P. Teubenbacher, M.P. Weigl, P. Kirchweger, D. Beitzke, A. Stiglbauer-Tscholakoff, A. Panzenböck, I. Lang, L.M. Mauracher, L. Hell, I. Pabinger, M.A. Bailey, D.J.A. Scott, L. Maegdefessel, A. Busch, I. Huk, C. Neumayer, C. Brostjan, Histone citrullination as a novel biomarker and target to inhibit progression of abdominal aortic aneurysms, Transl. Res. 233 (2021) 32–46.
- [46] C. Thålin, M. Daleskog, S.P. Göransson, D. Schatzberg, J. Lasselin, A.C. Laska, A. Kallner, T. Helleday, H. Wallén, M. Demers, Validation of an enzyme-linked immunosorbent assay for the quantification of citrullinated histone H3 as a marker for neutrophil extracellular traps in human plasma, Immunol. Res. 65 (3) (2017) 706–712.
- [47] P. Jiang, C.W. Chan, K.C. Chan, S.H. Cheng, J. Wong, V.W. Wong, G.L. Wong, S. L. Chan, T.S. Mok, H.L. Chan, P.B. Lai, R.W. Chiu, Y.M. Lo, Lengthening and shortening of plasma DNA in hepatocellular carcinoma patients, Proc. Natl. Acad. Sci. U. S. A. 112 (11) (2015) E1317–E1325.
- [48] R. Zhang, K. Nakahira, X. Guo, A.M. Choi, Z. Gu, Very short mitochondrial DNA fragments and heteroplasmy in human plasma, Sci. Rep. 6 (2016), 36097.
- [49] E. Hazkani-Covo, R.M. Zeller, W. Martin, Molecular poltergeists: mitochondrial DNA copies (numts) in sequenced nuclear genomes, PLoS Genet. 6 (2) (2010), e1000834.
- [50] A.N. Malik, A. Czajka, Is mitochondrial DNA content a potential biomarker of mitochondrial dysfunction? Mitochondrion 13 (5) (2013) 481–492.
- [51] S. Schubert, S. Heller, B. Löffler, I. Schäfer, M. Seibel, G. Villani, P. Seibel, Generation of rho zero cells: visualization and quantification of the mtDNA depletion process, Int. J. Mol. Sci. 16 (5) (2015) 9850–9865.
- [52] X. Li, G. Zhao, J. Zhang, Z. Duan, S. Xin, Prevalence and trends of the abdominal aortic aneurysms epidemic in general population—a meta-analysis, PLoS One 8 (12) (2013). e81260.
- [53] B. Zagrapan, W. Eilenberg, S. Prausmueller, P. Nawrozi, K. Muench, S. Hetzer, V. Elleder, R. Rajic, F. Juster, L. Martelanz, H. Hayden, J. Klopf, C. Inan, P. Teubenbacher, M.P. Weigl, P. Kirchweger, D. Beitzke, B. Jilma, J. Wojta, M. A. Bailey, D.J.A. Scott, I. Huk, C. Neumayer, C. Brostjan, A novel diagnostic and prognostic score for abdominal aortic aneurysms based on D-dimer and a comprehensive analysis of myeloid cell parameters, Thromb. Haemostasis 119 (5) (2019) 807–820.
- [54] H.G. Claycamp, Phenol sensitization of DNA to subsequent oxidative damage in 8hydroxyguanine assays, Carcinogenesis 13 (7) (1992) 1289–1292.
- [55] M.T. Finnegan, K.E. Herbert, M.D. Evans, J. Lunec, Phenol isolation of DNA yields higher levels of 8-oxodeoxyguanosine compared to pronase E isolation, Biochem. Soc. Trans. 23 (3) (1995) 430s.
- [56] H.J. Helbock, K.B. Beckman, M.K. Shigenaga, P.B. Walter, A.A. Woodall, H.C. Yeo, B.N. Ames, DNA oxidation matters: the HPLC-electrochemical detection assay of 8oxo-deoxyguanosine and 8-oxo-guanine, Proc. Natl. Acad. Sci. U. S. A. 95 (1) (1998) 288–293.
- [57] A. Klungland, I. Rosewell, S. Hollenbach, E. Larsen, G. Daly, B. Epe, E. Seeberg, T. Lindahl, D.E. Barnes, Accumulation of premutagenic DNA lesions in mice defective in removal of oxidative base damage, Proc. Natl. Acad. Sci. U. S. A. 96 (23) (1999) 13300–13305.

- [58] J.L. Ravanat, T. Douki, P. Duez, E. Gremaud, K. Herbert, T. Hofer, L. Lasserre, C. Saint-Pierre, A. Favier, J. Cadet, Cellular background level of 8-oxo-7,8-dihydro-2'-deoxyguanosine: an isotope based method to evaluate artefactual oxidation of DNA during its extraction and subsequent work-up, Carcinogenesis 23 (11) (2002) 1011, 1018
- [59] C. Badouard, Y. Ménézo, G. Panteix, J.L. Ravanat, T. Douki, J. Cadet, A. Favier, Determination of new types of DNA lesions in human sperm, Zygote 16 (1) (2008) 9–13
- [60] A. Grzelak, B. Rychlik, G. Bartosz, Light-dependent generation of reactive oxygen species in cell culture media, Free Radic. Biol. Med. 30 (12) (2001) 1418–1425.
- [61] J.A. Nicklas, E. Buel, Simultaneous determination of total human and male DNA using a duplex real-time PCR assay, J. Forensic Sci. 51 (5) (2006) 1005–1015.
- [62] K. Funakoshi, M. Bagheri, M. Zhou, R. Suzuki, H. Abe, H. Akashi, Highly sensitive and specific Alu-based quantification of human cells among rodent cells, Sci. Rep. 7 (1) (2017), 13202.
- [63] N. Witt, G. Rodger, J. Vandesompele, V. Benes, A. Zumla, G.A. Rook, J.F. Huggett, An assessment of air as a source of DNA contamination encountered when performing PCR, J. Biomol. Tech. 20 (5) (2009) 236–240.
- [64] H. Kaur, B. Halliwell, Measurement of oxidized and methylated DNA bases by HPLC with electrochemical detection, Biochem. J. 318 (Pt 1) (1996) 21–23.
- [65] O. Espinosa, J. Jiménez-Almazán, F.J. Chaves, M.C. Tormos, S. Clapes, A. Iradi, A. Salvador, M. Fandos, J. Redón, G.T. Sáez, Urinary 8-oxo-7,8-dihydro-2'-deoxyguanosine (8-oxo-dG), a reliable oxidative stress marker in hypertension, Free Radic. Res. 41 (5) (2007) 546–554.
- [66] S. Loft, H.E. Poulsen, Cancer risk and oxidative DNA damage in man, J. Mol. Med. 74 (6) (1996) 297–312.
- [67] M.K. Shigenaga, C.J. Gimeno, B.N. Ames, Urinary 8-hydroxy-2'-deoxyguanosine as a biological marker of in vivo oxidative DNA damage, Proc. Natl. Acad. Sci. U. S. A. 86 (24) (1989) 9697–9701.
- [68] C.S. Lin, L.S. Wang, C.M. Tsai, Y.H. Wei, Low copy number and low oxidative damage of mitochondrial DNA are associated with tumor progression in lung cancer tissues after neoadjuvant chemotherapy, Interact. Cardiovasc. Thorac. Surg. 7 (6) (2008) 954–958.
- [69] X.B. Wang, N.H. Cui, X. Liu, X. Liu, Mitochondrial 8-hydroxy-2'-deoxyguanosine and coronary artery disease in patients with type 2 diabetes mellitus, Cardiovasc. Diabetol. 19 (1) (2020) 22.
- [70] J.E. Bajacan, I.S. Hong, T.M. Penning, M.M. Greenberg, Quantitative detection of 8-Oxo-7,8-dihydro-2'-deoxyguanosine using chemical tagging and qPCR, Chem. Res. Toxicol. 27 (7) (2014) 1227–1235.
- [71] N. Mehra, M. Penning, J. Maas, N. van Daal, R.H. Giles, E.E. Voest, Circulating mitochondrial nucleic acids have prognostic value for survival in patients with advanced prostate cancer, Clin. Cancer Res. 13 (2 Pt 1) (2007) 421–426.
- [72] G. Fanò, P. Mecocci, J. Vecchiet, S. Belia, S. Fulle, M.C. Polidori, G. Felzani, U. Senin, L. Vecchiet, M.F. Beal, Age and sex influence on oxidative damage and functional status in human skeletal muscle, J. Muscle Res. Cell Motil. 22 (4) (2001) 345–351.
- [73] M. Pinti, E. Cevenini, M. Nasi, S. De Biasi, S. Salvioli, D. Monti, S. Benatti, L. Gibellini, R. Cotichini, M.A. Stazi, T. Trenti, C. Franceschi, A. Cossarizza, Circulating mitochondrial DNA increases with age and is a familiar trait: implications for "inflamm-aging", Eur. J. Immunol. 44 (5) (2014) 1552–1562.
- [74] A. Siomek, D. Gackowski, R. Rozalski, T. Dziaman, A. Szpila, J. Guz, R. Olinski, Higher leukocyte 8-oxo-7,8-dihydro-2'-deoxyguanosine and lower plasma ascorbate in aging humans? Antioxid. Redox Signal. 9 (1) (2007) 143–150.
- [75] R. Guevara, M. Gianotti, J. Oliver, P. Roca, Age and sex-related changes in rat brain mitochondrial oxidative status, Exp. Gerontol. 46 (11) (2011) 923–928.
- [76] S. Asami, H. Manabe, J. Miyake, Y. Tsurudome, T. Hirano, R. Yamaguchi, H. Itoh, H. Kasai, Cigarette smoking induces an increase in oxidative DNA damage, 8hydroxydeoxyguanosine, in a central site of the human lung, Carcinogenesis 18 (9) (1997) 1763–1766.
- [77] P.K. Ellegaard, H.E. Poulsen, Tobacco smoking and oxidative stress to DNA: a metaanalysis of studies using chromatographic and immunological methods, Scand. J. Clin. Lab. Invest. 76 (2) (2016) 151–158.
- [78] D. Brea, J. Roquer, J. Serena, T. Segura, J. Castillo, Oxidative stress markers are associated to vascular recurrence in non-cardioembolic stroke patients non-treated with statins, BMC Neurol. 12 (2012) 65.
- [79] Y.S. Li, M.F. Song, H. Kasai, K. Kawai, 8-hydroxyguanine in urine and serum as an oxidative stress marker: effects of diabetes and aging, J. UOEH 35 (2) (2013) 119–127.
- [80] C.S. Shin, B.S. Moon, K.S. Park, S.Y. Kim, S.J. Park, M.H. Chung, H.K. Lee, Serum 8-hydroxy-guanine levels are increased in diabetic patients, Diabetes Care 24 (4) (2001) 733–737.
- [81] A.L. Price, E. Eskin, P.A. Pevzner, Whole-genome analysis of Alu repeat elements reveals complex evolutionary history, Genome Res. 14 (11) (2004) 2245–2252.
- [82] B. Zagrapan, W. Eilenberg, A. Scheuba, J. Klopf, A. Brandau, J. Story, K. Dosch, H. Hayden, C.M. Domenig, L. Fuchs, R. Schernthaner, R. Ristl, I. Huk, C. Neumayer, C. Brostjan, Complement factor C5a is increased in blood of patients with abdominal aortic aneurysm and has prognostic potential for aneurysm growth, J. Cardiovasc. Transl. Res. 14 (4) (2021) 761–769.